AIMS Environmental Science

AIMS Environmental Science, 6(6): 472–482.
DOI: 10.3934/environsci.2019.6.472
Received: 31 August 2019
Accepted: 20 November 2019
Published: 04 December 2019

http://www.aimspress.com/journal/environmental

Research article

Characterization of high background radiation of terrestrial naturally occurring radionuclides in a mining region of Senegal

Mamadou Lamine Sane*, Modou MBAYE, Djicknack Dione and Ahmadou Wague

Institute of Applied Nuclear Technology, Faculty of Sciences and Techniques, University of Cheikh Anta Diop, P.O. Box 5005, Dakar, Senegal

*** Correspondence:** Email: mamadou2.sane@ucad.edu.sn; Tel: +221775488420.

Abstract: A survey of natural radioactivity has been carried out to estimate the concentration of naturally occurring radionuclides and radiological risk associated in the south East mining region, which present high natural background radiation. An in-situ gamma-ray spectrometer was used to map natural environmental gamma-emitting radionuclides. A combined inferential statistical and chemometrics of naturally occurring radionuclides were used for data modelling and characterization. The radiological data surveys were explored using inferential statistical, principal component analysis and a supervised support vector machine learning. First, one-way Analysis of variance, on-parametric Kruskal Wallis test, was applied allowing pairwise comparison of radionuclides levels in sampling sites, second, data was submitted to PCA to extract noise-free data and reduced data was analyzed with support vector machine. PCA results show that ^{238}U contribution (56%) is dominant in the first principal component with ^{40}K (35%). The second component, with the cumulative variance explained of 88%, is dominated by ^{232}Th (68%) and ^{40}K (31%). Anova indicates that there is a significant difference in the mean mass concentration of samples type and soil activities are mostly lower. The best classification accuracy was 100% with the use of radial kernel density function. As potential uranium and gold mine site, these results will allow establishing both reference values for background radiation of the region and fingerprinting sources of naturally occurring radionuclides.

Keywords: Potassium-40; Thorium-232; Uranium-238; gamma spectrometry; radiological hazard

1. Introduction

Primordial radionuclides and their decay products are radioisotopes that represent a potential risk for human due to the emission of high-energy ionizing radiation. Naturally gamma-emitting radioisotopes are the principal source of outdoors exposition and it is responsible for approximately between 80% and 85% gamma radiation received by humans. Exposition, mainly, arises from ^{238}U, ^{232}Th and ^{40}K decay daughters (radium and radon). Based on UNSCEAR, in average ^{40}K contributes 13.8%, ^{232}Th 14% and ^{238}U to 55% to the worldwide terrestrial gamma dose of 60 nGyh^{-1} [1]. Eastern Senegal has an important and wide variety of mineral substances including precious metals such as gold, heavy minerals (zircon), building material and ornamental stones. The search of Uranium has been launched at the beginning of 2007 and an exploitation overs decade in the east Saraya region induces tremendous visible environmental impacts including both mechanical and chemical weathering. Nowadays environmental monitoring of radioactivity in soils, rocks, air and superficial water, as well as their fate in the environment, is an increasing demand for policymakers; and more importantly, it has been demonstrated that quantification of background levels of radionuclides is necessary to evaluate the potential environmental risk [2]. According to existing literature, measurement of concentration in soil of ^{238}U, ^{232}Th and ^{40}K have been performed in a number of countries all around the world [3–13]. However, there are very few data available of naturally occurring radionuclides in soil from developing countries due to the cost of radioactivity monitoring and time-consuming existing methodologies [14]. Based on our knowledge, in our study area, there is no reference radiological hazard-monitoring program, despite the existence of many industrial and artisanal mines.

Portable gamma-ray spectrometer is widely used for environmental studies. It offers a rapid and cost-effective In-situ assessment of gamma emitter's radionuclides in rocks and soil. The present study has been carried out to assess the specific activities concentration of some terrestrial gamma-emitting radionuclides and to evaluate the radiation radiological value of ^{40}K, ^{232}Th and ^{238}U. In addition, we report the results of the utility of inferential statistical, principal component analysis and a supervised support vector machine learning for accurate fingerprinting of naturally occurring radionuclides sources from different samples. This result is also contributing to establishing a baseline level of natural radioactivity and to assess radiation doses in the mining region of Senegal.

2. Material and methods

The study area was the district of Saraya in the region of Kedougou, southern-east of Senegal, located at coordinates (12°50'35.24"N – 12°51'57.86"N; 11°46'19.12"W – 11°47'58.55"W). This site is located off one of the major uranium deposits in Senegal that is the mining region where a high level of natural radioactivity has been measured many years ago. Figure 1 shows the geographic location of the study area. The study area is characterized by cumulative rain between 1100 and 1500 mm in the time period between 2015–2016. Local temperature varies substantially between 19 °C to 45 °C.

A high resolution, 1024 channels portative gamma spectrometer with a large (103 cm^3) high-density Bismuth Germanate (BGO) crystal detector with an energy range between 30Kev to 3000Kev, was used for field measurement. The sampling Measurement time was set around 5 minutes for each individual point in a pseudo-randomly sampling procedure. A Bluetooth GPS device paired with the spectrometer was used to record the geographical position. The gamma-ray spectra recorded for each

point were further analyzed and taking into account transition of interest from well-defined photo peak from natural radioisotopes of ^{40}K, ^{232}Th and ^{238}U. Determination of the primordial potassium ^{40}K in soil was through the detection of 1460Kev of associated with the gamma-ray decay of ^{40}K. Based on the assumption of secular equilibrium of naturally occurring radioisotopes of ^{232}Th and ^{238}U primordial series; the thorium radioisotope was estimated through the detection of 2615Kev gamma ray energy of ^{208}TI; similarly, ^{238}U was estimated through detection of 1765Kev gamma ray energy of ^{214}Bi. An assumption of equilibrium of primordial radionuclides is common in rocks and the ^{232}Th series may be considered in equilibrium in most geological environments [15]. The activity concentration of radioisotopes was converted into specific concentration according to the following relation given by UNSCEAR 2000.

1% K= 313 $Bqkg^{-1}$ ^{40}K

1 ppm U=12.25 $Bqkg^{-1}$ ^{238}U

1 ppm Th= 4.06 $Bqkg^{-1}$ ^{232}Th

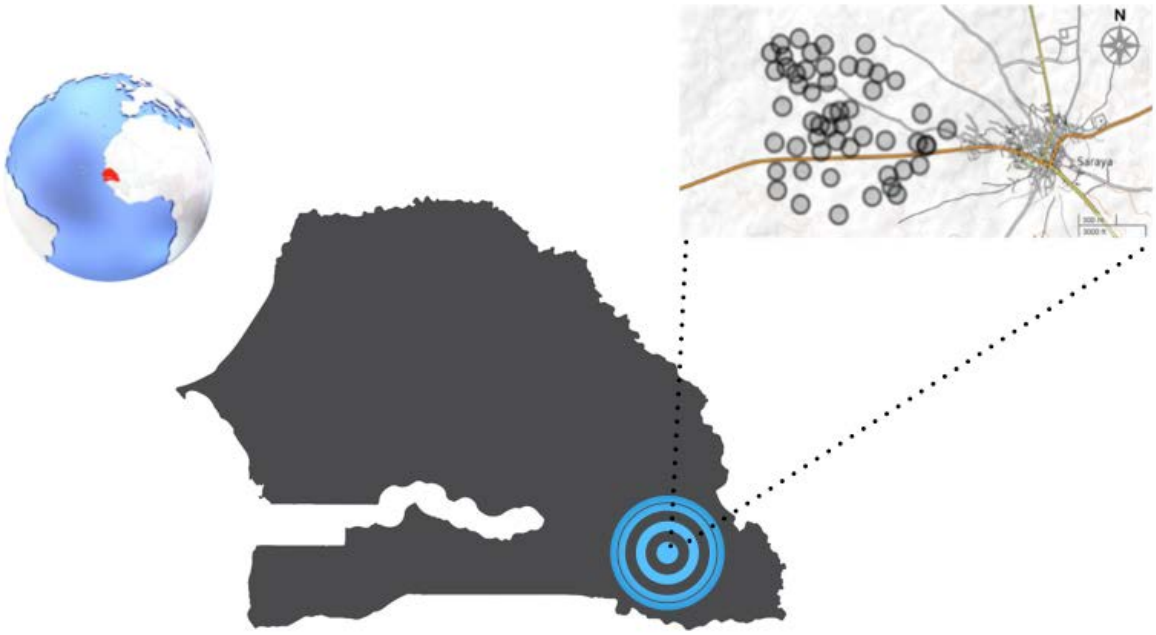

Figure 1. Study site in the eastern south of Senegal, which is the principal mining region in Senegal. A random sampling strategy was conducted.

2.1. Radiological risk assessment

NORs are well known to cause a significant increase in public exposition. In this study, four radiological hazard indices associated with the presence the measured naturally occurring radioactive materials were computed using conversion factors. Equations 1 to 4 expressed the following radiological risk index.

1. The total absorbed dose rate in air
2. The radium equivalent index
3. The External hazard index
4. The annual effective dose equivalent

Average specific activity of radioisotopes was converted into dose rate using Eq 1 given by:

$$D[nGyh^{-1}] = \alpha A_U + \beta A_{Th} + \lambda A_K \quad (1)$$

where D (nGyh^{-1}) is the external terrestrial γ-radiation absorbed dose rate in air at a height of about 1 meter above the ground and α(0.462), β(0.604) and λ(0.0417) are given dose conversion factors and A_U, A_{Th} and A_K are specific mass activity of ^{238}U,^{232}Th and ^{40}K. Equation is based on secular equilibrium of primordial radioisotopes U-series and Th-series. Based on the specific activity of ^{40}K, ^{232}Th and ^{238}U in soil, their resulting Uranium activities equivalent were using Eq 2 according Gonzalez-Fernandez et al. [16]. Equation 2 is based on the assumption that 10 Bqkg^{-1} of ^{238}U produce the same gamma radiation dose rate as 7 Bqkg^{-1} of ^{232}Th and 130 Bqkg^{-1} of ^{40}K.

$$Ra_{eq}[BqKg^{-1}] = A_U + \eta A_{Th} + \zeta A_K \quad (2)$$

where A_U, A_{Th} and A_k are the specific activity in Bqkg^{-1} of Uranium, thorium and potassium respectively. η (1.43) and ζ (0.077) are conversion factor. The external hazard index due to external gamma radiation exposure is given by Eq 3.

$$H_{ex} = \varphi A_U + \mu A_{Th} + \tau A_K \leq 1 \quad (3)$$

where A_U, A_{Th} and A_k are the specific activity in Bqkg^{-1} of radium, thorium and potassium respectively. $\varphi\left(\frac{1}{370}\right)$ $\mu(\frac{1}{259})$ and $\tau(\frac{1}{4810})$ are conversion factor.

The indoor annual effective dose hazard index was expressed as follow:

$$Indoor[nSv] = D(nGyh^{-1}) \times 8.760(h) \times 0.8 \times 0.7(SvGy^{-1}) \quad (4)$$

where D is the absorbed dose; 0.7 SvGy^{-1} is used for the conversion coefficient from absorbed dose in air to effective dose received by adults and 0.8 for the indoor occupancy factor, i.e. the fraction of time spent indoors and outdoors is 0.8 and 0.2, respectively according to UNSCEAR 2000.

2.2. Principal component analysis

Principal component analysis (PCA) is a widely unsupervised learning method for data visualization, data reduction, and pre-processing prior to the application of supervised multivariate techniques [17–19]. PCA algorithm finds a low-dimensional representation of the data with as much as possible of variance. Each dimension is a linear combination of the p-variable given by Eq 5 and the principal components are obtained by solving the optimization problem given by Eq 6.

$$t_{iI} = \sum_{p=1}^{3} p_p x_{ip} \quad (5)$$

$$Maximize\left\{\frac{1}{n}\sum_{i}^{n}\left(\sum_{j=1}^{p} p_p\, x_{ip}\right)^2\right\} \quad (6)$$

where p_p are the loadings of the p^{th}-principal component axis with $p_p p_p^T = 1$ or and t_{iI} are the score which express the linear combination of loading and variables x_{ip}. The initial data matrix can be reconstructed with reduced noise from the scores, T and loading with correspond to the main structure of the data with maximum variance explain. The noise free reconstruction matrix is given by Eq 7.

$$\tilde{X} = TP^t \tag{7}$$

2.3. Support vector machine

SVM classifier is a widely used statistical tool for classification and regression and efficient method to model complex data with the use of a class of Kernel function. The objective of SVM is to develop a classifier based on the training data and perform perfect group separation for all the sample type to their class y {−1, 0, +1}, from n dimensional input data represented by a vector written x = (x_1, $x_{2...}x_n$) in the case of 3-class classification problem. Detail technical description of SVM algorithm can be found elsewhere [20]. In our study we applied a non-linear boundaries classification with a radial kernel density estimation given by Eq 8.

$$\mathrm{K}(x_{ij}, x'_{ij}) = e^{-(\gamma \sum_{j=1}^{p}\left(\left[x_{ij} - x'_{ij}\right]^2\right)} \tag{8}$$

where $\left[x_{ij} - x'_{ij}\right]^2$ is a Euclidean distance estimated with paired observations and γ is a positive constant. P is the number of training observation used in the model.

3. Results and discussion

3.1. Radiological hazard

Table 1 summarizes descriptive statistics of the radiological hazard assessment in this study. As shown in Table 1, the radiological equivalent index for all sample type ranged between 83 and 384.9 Bqkg^{-1} with a arithmetic mean about 181 Bqkg^{-1}, in some point sample the Ra_{eq} is higher than the recommended maximum value of 370 Bqkg^{-1}. Similarly, the calculated external hazard index varied between 0.22 and 1.04 Bqkg^{-1} with an arithmetic mean 0.49 Bqkg^{-1}and a maximum value $H_{ex} > 1$ found is exclusively due to rock sample. 63% of the value of Hex due to rock was found to have Hex greater than 0.5 Bqkg^{-1} while vegetation sample contributed around 34.70% and soil samples sample about 2.30%. The absorbed gamma dose highest value was about 177 nGyh^{-1} which is 3 times higher than the world average outdoor gamma dose. The annual effective Indoor estimated gamma radiation value ranged between 0.19 mSv and 0.87 mSv and the arithmetic mean and standard error are about 0.43 and 0.01 mSv, respectively.

Table 1. Descriptive statistics of radiological hazard assessment including the Radium equivalent index (Ra_{eq}), the External Hazard index (*Hex*), and the gamma absorbed dose (*D*) and the annual effective indoor dose. The descriptive parameter include standard deviation (sd) the skewness (skew) of the data set and the standard error (se).

	Ra_{eq}	H_{ex}	*D*	Indoor
	($Bqkg^{-1}$)	($Bqkg^{-1}$)	($nGyh^{-1}$)	(mSv)
Mean	181.69	0.49	86.74	0.43
sd	65.18	0.18	29.77	0.15
Minimum	83	0.22	37.95	0.19
Maximum	384.90	1.04	177.77	0.87
skew	0.78	0.78	0.67	0.67
se	2.88	0.01	1.31	0.01

3.2. Kruskall Wallis test

The descriptive statistics (mean, minimum, maximum and standard error) of naturally occurring radionuclides are given in Figure 2. Prior to application of statistical inference, the activity concentration data were submitted to a statistical test for homogeneity of variance (F-test) and for normally (Shapiro-Wilk test). Whenever both conditions were satisfied, a parametric t-test was applied otherwise; a non-parametric Wilcoxon-Mann-Whitney test was used. The level of significance of the test was set at 5%. The mass activity concentration of ^{40}K found varied differently within and among samples. They ranged from 187 to 1471 $Bqkg^{-1}$ in rock, between 219 and 1283 $Bqkg^{-1}$ in soil and between 125 and 1533 $Bqkg^{-1}$ in vegetation. The variability of the radionuclide ^{40}K in soil was relatively small (sd = 156 $Bqkg^{-1}$) compared vegetation (sd = 217 $Bqkg^{-1}$) and rock (sd = 286 $Bqkg^{-1}$). ANOVA shows the significant statistical difference between ^{40}K concentration among sites (Wilcoxon-Mann-Whitney, $p < 0.001$) and the concentration in grass vegetation was statistically higher. Similarly, ^{238}U were significantly different among samples (Wilcoxon-Mann-Whitney, $p < 0.001$) and its value in rock (150 ± 72) as expected was higher in soil (40 ± 17) and vegetation (58 ± 24). However, there was no significant difference in the ^{232}Th mass concentration different between soil and vegetation (Wilcoxon test with Benforrri Adjust P-values for Multiple Comparisons, $p > 0.05$)

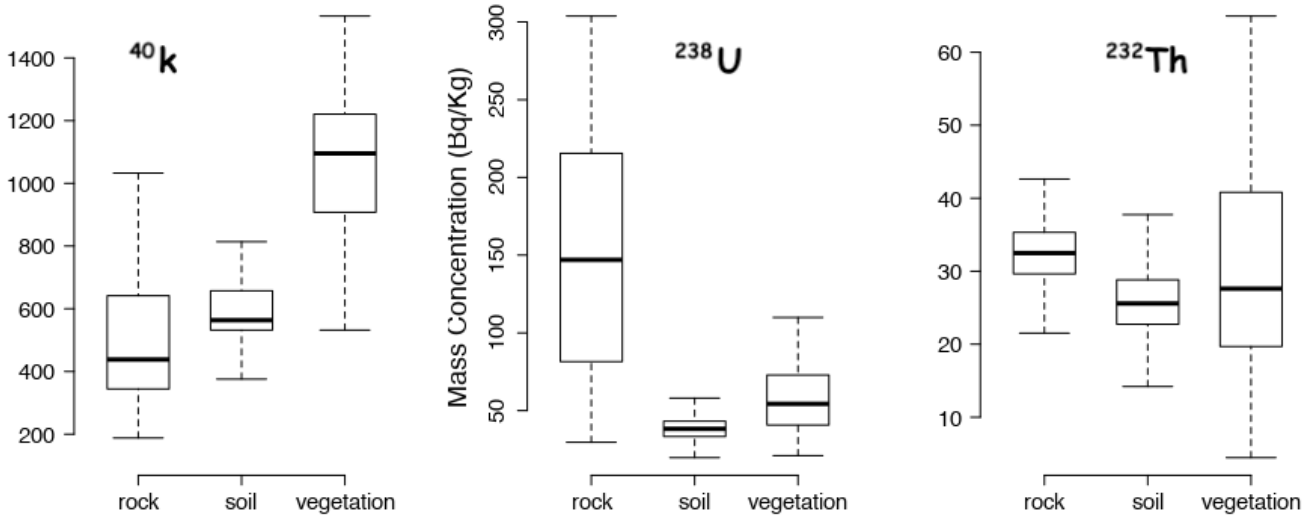

Figure 2. Boxplot displaying activities concentration as function of sampling site.

3.3. Principle component analysis

Unsupervised PCA was used to study to extract radiological signature underlining naturally occurrence of ^{232}Th, ^{238}U and ^{40}K. In our study, the raw data consists of 513 points measurement, 3 quantitative radionuclides and 1 qualitative variable, which describe field-sampling type. The data submitted to principal component analysis was centered and reduced to unit variance to attribute each radionuclide equal weight. Table 2 displays the loading or contribution of each radionuclide and the v-test which indicates whether a qualitative variable (soil, rock, vegetation) characterize a component [21]. Table 2 shows that ^{238}U contribution (56%) is dominant in the first principal component (PC1) axis as well as ^{40}K (35%) while ^{232}Th have an approximately null contribution on PC1 (9%). The second component is dominated by ^{232}Th (68%) and ^{40}K (31%). 50% of the total variance explained is represented by first principal component (PC1), while PC2 counts for 38% of the total variance. PC1 corresponds to the measure of the alteration and erosion component. Indeed, Potassium is mostly affected by weathering of rock, distributed by erosion processes on soil and it is efficiently uptake by clay soil and plants, this is demonstrated by the contribution of ^{40}K in both PC1 and PC2 and the high value of their coefficient of variation ^{40}K(44%) and ^{238}U (79%). However, ^{232}Th (68%) contribute dominantly to the second component axis. The contribution of ^{232}Th PC2 could be described as a measure of stability. ^{232}Th is almost identically distributed among sites and it is less affected by weathering process. In addition, the coefficient of variation is less important (28%), less variability among samples.

Table 2. Contribution of each radionuclides in the first two principal components and the measure of rock, soil and vegetation in the components.

	Contribution (%)			v-test		
	^{40}K	^{238}U	^{232}Th	Rock	Soil	Veg
PC1	35	56	9	16	−5	−11
PC2	31	1	68	0.8	−9	8

As indicated in Table 2, soil sample has no effect on the principal component axis construction (negative v-test in all two dimensions), while rock (v-test = 12) and vegetation (v-test = 5) characterize the first and second principal component (PC1 and PC2). Figure 3 displays both the principal component scores and the loading vectors in a single bi-plot. As presented in Figure 3, radiological environmental variables ^{40}K, ^{238}U and ^{232}Th are not positively correlated. It is noted that ^{40}K and ^{238}U are completely independent among samples (variables are orthogonally related).

As the application of principal component analysis on the raw data did not show clear discrimination of samples despite the cumulative variance of 88%, further processing has been done using matrix reconstruction and inferential statistics. Based on the non-parametric variance analysis result that demonstrated that there was no significant statistical difference between thorium level in soil and vegetation, we applied a raw data transformation by extracting vegetation raw data and dividing each variable by the Thorium activity mass concentration. Figure 3b shows the results on PCA on transformed-reconstruction matrix data with a total of 98% of variability explained by the first 2 principal components axis. From the transformed data bi-plot shown in Figure 3b, it may be observed that the samples may be classified with an unsupervised technique combined with ANOVA inference.

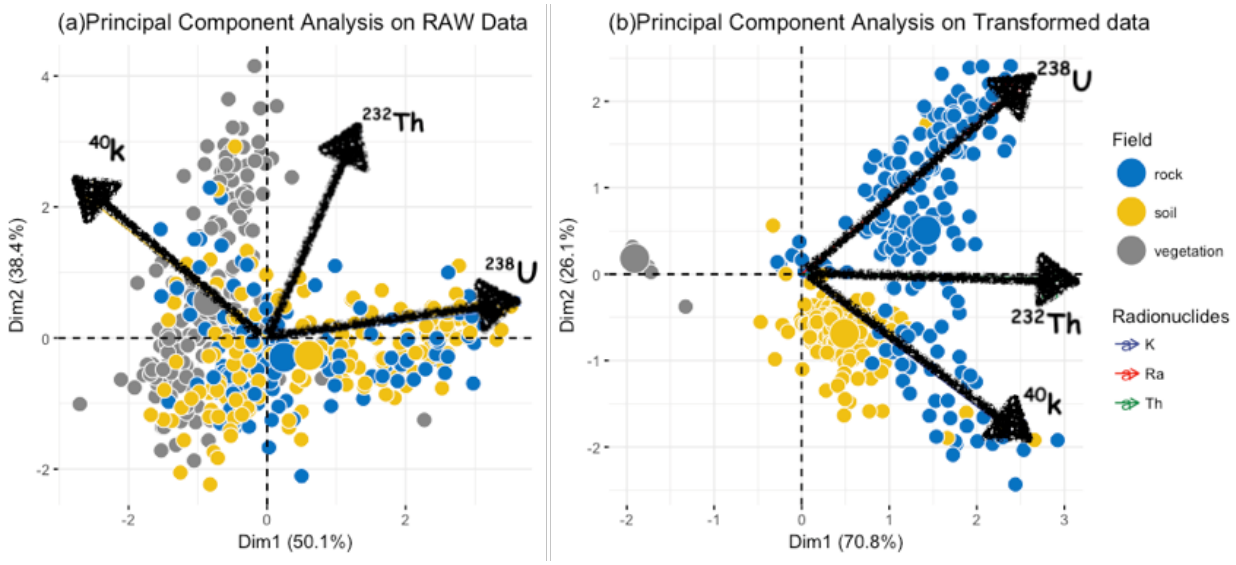

Figure 3. Principal component analysis of naturally occurring radionuclides with (a) a scaled variables for unit variance of the raw data set and (b) the transformed data based on inferential statistics.dim1 and dim2 referred to principal components.

3.4. Support vector machine learning

All samples in the dataset are divided into two sets, the training set includes 62% of the samples and the test set includes 38% of the total samples. Prior to application of SVM, a 10-fold cross-validation was performed to tune the model and to estimate the best parameters to include in the classification model. The model parameters are given in Table 6, which displays the results of the cross-validation tuning of the model parameters (cost function, cross-validation error and error dispersion). The parameters (error = 0.31 and cost = 1) are the one used for the SVM.

Table 4. Ten-fold cross-validation for best parameters model estimated of the cost function, the error and the dispersion. All the statistical analysis was performed with R software.

Cost	Error	Dispersion
0.001	0.756	0.048
0.01	0.411	0.078
0.1	0.166	0.050
0.8	0.154	0.047
1	0.152	0.048
1.5	0.154	0.049
2	0.154	0.051
3	0.162	0.050
4	0.160	0.052
5	0.158	0.050
6	0.156	0.051
7	0.156	0.051
8	0.156	0.051
9	0.158	0.053
10	0.158	0.053

Figure 4 shows the result of the non-linear radial kernel support vector machine classification. The best classification accuracy was 100% that gives neat separation of the three categories of samples based on the measured terrestrial naturally occurring radionuclides.

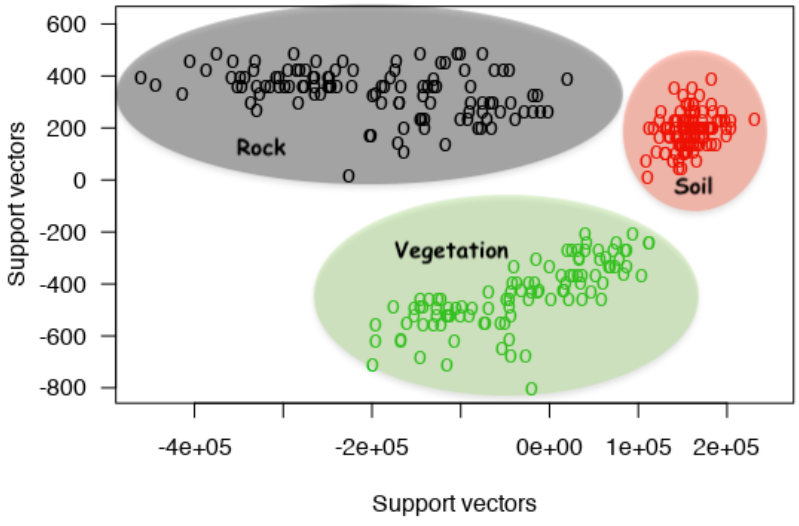

Figure 4. Support vector machine SVM classification with a radial kernel density function of 3 classes vegetation, rock and soil of naturally occurring radionuclides variables.

4. Conclusion

In this study, we demonstrated that the use of in-situ gamma-ray spectrometric measurements combined with inferential statistics and support vector machine has high potential to fingerprint

sources of naturally occurring radionuclides. The Radial kernel SVM classifiers achieved the best identification of the three sources with 100% of accuracy. Unsupervised principal component analysis, on both raw and the transformed data was not able to make a net separation among samples. It can be concluded that the level of natural radionuclide activity concentrations is mostly influenced by weathering and erosion process. We also establish the reference values for background radiation of the major mining region. In addition, the absorbed gamma dose highest value was about 3 times higher than the world average outdoor gamma dose.

Acknowledgements

The authors would like to thank the members of the Laboratory of Applied Remote Sensing, LTA, and the Institute for Applied Nuclear Technology for their comments and discussions. They express their gratitude to the Department of Geology of the Cheikh Anta Diop University of Dakar for their availability the Gamma spectrometer which allowed us to make measurements. The authors would like to thank Prof David Baratoux and Dr. Makhoudia Fall for their collaboration.

Conflict of interest

The authors declare no conflict of interest.

Reference

1. UNSCEAR (2000) United Nations Scientific Committee on the Effects of Atomic Radiation. Report to the General Assembly, with Scientific Annexes. Sources and effects and risks of ionizing radiation. United Nations. New York.
2. Latife S, Nurgül H, Hakan Ç (2017) Assessment of radiological hazard parameters due to natural radioactivity in soils from granite-rich regions in Kütahya Province, Turkey. *Isot Environ Healt S* 53: 212–221.
3. Alam M, Miah M, Chowdhury M, et al. (2016) Attenuation coefficients of soils and some building materials of Bangladesh in the energy range 276–1332 keV. *Appl Radiat Isotopes* 54: 973–6.
4. Faheem M, Mujahid S, Matiullah M (2008) Assessment of radiological hazards due to the natural radioactivity in soil and building material samples collected from six districts of the Punjab province, Pakistan. *Radiat Meas* 43: 1443–7.
5. Kapdan E, Altinsoy N, Karahan G (2011) Determination of the health hazards due to background radiation sources in the city of Adapazari, Northwestern Turkey. *Isot Environ Healt S* 47: 93–100.
6. Khan HM, Ismail M, Zia MA (2012) Measurement of radionuclides and absorbed dose rates in soil samples of Peshawar, Pakistan, using gamma ray spectrometry. *Isot Environ Healt S* 48: 295–301.
7. Yang Y, Wu X, Jiang Z (2005) Radioactivity concentrations in soils of the Xiazhuang granite area, China. *Appl Radiat Isotopes* 63: 255–9.
8. Dione D, Mbaye M, Sané ML, et al. (2018) Survey of Activity Concentration and Dose Estimation of Naturally Occurring Radionuclides (232Th, 238U and 40K) in the Coastal area of Dakar, Senegal. *Indian J Sci Tech* 11: 1–7.
9. Krstic D, Nikezic D, Stevanovic N, et al. (2007) Radioactivity of some domestic and imported building materials from South Eastern Europe. *Radiat Meas* 47: 1731–1736.

10. El-Arabi A, Abbady A, El-Hussein A (2011) Gamma-ray measurements of natural radioactivity in sedimentary rocks from Egypt. *Nucl Sci Tech* 17: 123–8.
11. Msaki P, Banzi FP (2000) Radioactivity in products derived from gypsum in Tanzania spectrometry. *Radiat Prot Dosim* 91: 409–12.
12. Navas A, Gaspar L, López-Vicente M, et al. (2011) Spatial distribution of Natural and artificial radionuclides at the catchment scale (South Central Pyrenees). *Radiat Meas* 46: 261–9.
13. Prakash MM, Kaliprasad CS, Narayana Y (2017) Study on natural radioactivity in the rocks of Coorg District, Karnataka State. *Radia Res J Appl Sci* 10: 128–134.
14. Safarov AA, Safarov AN, Azimov AN, et al. (2017) Rapid assessment methodology in NORM measurements from building materials of Uzbekistan. *J Environ Radioactiv* 169: 186–191.
15. Chiozzi P, Pasquale V, Verdoya M (2002) naturally occurring radioactivity at the Alpsapennines transition. *Radia Meas* 35: 147–154.
16. Gongàlez-Fernàndez AB, Marcelo V, Valenciano JB, et al. (2012) Relationship between physical and chemical parameters for four commercial grape varieties from the Bierzo region (Spain). *Sci Hortic* 147: 111–117.
17. Mbaye M, Traore A, Ndao AS, et al. (2015) Multivariate Statistical Techniques to Determine Essential and Toxic Elements in Biological Samples by X-Ray Fluorescence. *Instrum Sci Technol* 43: 369–378.
18. Varmuza K, Filzmoser P (2016) Introduction to Multivariate Statistical Analysis in Chemometrics. CRC Press, Florida.
19. Mabit L, Gibbs M, Mbaye M, et al. (2018) Novel application of Compound Specific Stable Isotope (CSSI) techniques to investigate on-site sediment origins across arable fields. *Geoderma* 316: 19–26.
20. Vapnik VN (1995) The Nature of Statistical Learning Theory, Springer-Verlag, New York.
21. Husson F, Lê S, Pagès J (2017) Exploratory Multivariate Data Analysis by Example Using R. Chapman & Hall/CRC Computer Science & Data Analysis (2nd edition).

AIMS Press